

## Ergodicity of a system with second-order phase transition: applicability of mode coupling theory

This article has been downloaded from IOPscience. Please scroll down to see the full text article.

1991 J. Phys.: Condens. Matter 3 9195

(<http://iopscience.iop.org/0953-8984/3/46/020>)

View [the table of contents for this issue](#), or go to the [journal homepage](#) for more

Download details:

IP Address: 171.66.16.96

The article was downloaded on 10/05/2010 at 23:50

Please note that [terms and conditions apply](#).

## Ergodicity of a system with second-order phase transition: applicability of mode coupling theory

W Kob†† and R Schilling§

† Institut für Physik, Universität Basel, Klingelbergstrasse 82 CH-4056 Basel, Switzerland

§ Institut für Physik, Johannes Gutenberg-Universität Mainz, Postfach 3980, D-6500 Mainz, Federal Republic of Germany

Received 3 January 1991, in final form 28 May 1991

**Abstract.** We investigate the applicability of mode coupling theory (MCT) to a system with a second-order phase transition. We have calculated numerically the time autocorrelation function of pseudo-spin variables for a  $\phi^4$ -model with infinite range interactions. In contrast to some Lennard-Jones liquids we do not find any evidence for an ergodic  $\rightarrow$  non-ergodic instability as predicted by Aksenov *et al* using MCT. We argue that this instability, at least for the  $\phi^4$ -model (with short- or long-range interactions), is a consequence of the approximations performed within the MCT. However, we stress that our results do not imply the same conclusion for supercooled liquids. The relaxation is non-Debye with a mean relaxation time  $\tau(T, N)$  ( $N$  is the number of atoms) exhibiting a rather unusual temperature dependence. In contrast to Arrhenius behaviour the relaxation becomes accelerated with decreasing temperature as long as  $T$  is sufficiently above the critical temperature  $T_c$ . For finite  $N$  our results indicate a scaling law  $\tau(T, N) = N\tau_0(T)$  for large  $N$ .

### 1. Introduction

There have been several attempts to account for the glass transition of structurally disordered materials like vitreous silica or metallic glasses. We do not discuss these theories here but the interested reader may consult, e.g., the review by Jäckle [1].

Recently a quite different approach was suggested to explain the transition from the supercooled liquid to a glassy state [2]. These contributions are based on mode coupling theory (MCT), originally devised to describe the critical dynamics at a second-order phase transition [3]. Studying the normalized time correlation function  $\phi_{\mathbf{q}}(t) = \langle \delta p_{\mathbf{q}}(t) \delta p_{\mathbf{q}}(0) \rangle / S_{\mathbf{q}}$  of the density fluctuations ( $\delta p_{\mathbf{q}}(t) = p_{\mathbf{q}}(t) - \langle p_{\mathbf{q}} \rangle$  with wavevector  $\mathbf{q}$ ,  $S_{\mathbf{q}}$  is the static structure factor and  $\langle \cdot \rangle$  denotes the average over the canonical ensemble), these authors have shown that a *dynamical transition* occurs at a temperature  $T_c^{\prime}$ ]. At this temperature the system changes from ergodic to non-ergodic behaviour, i.e. below  $T_c^{\prime}$  the correlation functions  $\phi_{\mathbf{q}}(t)$  no longer decay to zero¶. This type of transition has been interpreted as a ‘glass transition’ singularity.

† Present address: Department of Chemistry, Stanford University, Stanford CA-94305, USA.

]] In order to avoid confusion with the critical temperature  $T_c$  we use  $T_c^{\prime}$ . For liquids  $T_c^{\prime}$  is usually denoted by  $T_c$ .

¶ Strictly speaking this property in general does *not* imply non-ergodicity, but only the absence of mixing. The contrary, however, is true i.e. non-ergodicity implies the absence of mixing (see e.g. [4]).

Note that  $T'_c$  should not be confused with the calorimetric glass transition temperature  $T_g$  as the latter is not well defined because it depends on the cooling rate. For supercooled liquids MCT predicts  $T_g < T'_c < T_m$ , with  $T_m$  the melting temperature. This sharp transition at  $T'_c$  is found in an *idealized* MCT where hopping processes are neglected. Taking these into account, the transition becomes smeared out, but may still be observable [5]. Although there has been some criticism of the applicability of MCT to the dense liquid regime [6] (which has been partially invalidated [7, 8]), recent experimental (e.g. [9]) and numerical (e.g. [10]) work show agreement with some of the predictions of MCT. A review of this subject including a careful analysis of the experimental data is given by Götze [8].

An idealized transition has also been found for a *facilitated kinetic Ising model* without interactions [11], for spin glass and Potts glass models [12] and for *orientational glasses* [13]. However, detailed Monte Carlo studies for the facilitated Ising model have not confirmed the kinetic singularity [14].

The motivation for *this* work is mainly to investigate the applicability of MCT to systems with a second-order phase transition and the existence of a dynamical transition or at least a signature of it. The  $\phi^4$ -model belongs to this class of systems and has been extensively used to describe structural phase transitions. Its Hamiltonian is as follows

$$H = \sum_l \left[ \frac{p_l^2}{2m} + V_0(x_l) \right] + \frac{1}{4} \sum_{kl} C_{kl} (x_k - x_l)^2. \quad (1a)$$

Here  $m$  is the mass of the atoms,  $x_l$  the *scalar* displacement of atom  $l$  at site  $\mathbf{R}_l$  of a three-dimensional lattice and  $C_{kl} = C(|\mathbf{R}_k - \mathbf{R}_l|)$  are the elastic constants. For the on-site interaction  $V_0$  we use a double well potential

$$V_0(x) = -\frac{A}{2}x^2 + \frac{B}{4}x^4 \quad (1b)$$

with  $A$  and  $B$  positive. Restriction to  $A > \sum_l C_{0l}$  limits our investigation to the *order-disorder regime*, which will turn out to be the most interesting case for our purpose. The reader who is interested in more details on this type of model, and more generally in structural phase transitions, is referred to the review by Bruce and Cowley [15]. MCT has also been applied to the model given by (1). Analogous to supercooled liquids an instability at  $T'_c > T_c$  has been found [16] for the correlation function

$$S_{kl}(t) = \langle u_k(t)u_l(0) \rangle \quad (2)$$

where  $u_k(t) = x_k(t) - \langle x_k \rangle$ . This result has been obtained in a single-site approximation for large enough coupling constants  $C_{kl}$  and assuming anisotropy, i.e.  $C_{kl}$  depends on the direction of  $\mathbf{R}_k - \mathbf{R}_l$ . Although the treatment [16] is quantum mechanical, the conclusion holds for the classical system as well.

Our recent numerical simulations of a *one-dimensional*  $\phi^4$ -like model for which the double well potential (1b) has been replaced by a *piecewise parabolic* (double-quadratic) one has not given any evidence of non-ergodic behaviour [17]. Since this finding may be an artifact due to the one-dimensionality, we will study here a three-dimensional  $\phi^4$ -model with infinite-range interactions. This can be easily achieved by choosing in (1a)

$$C_{kl} \equiv \frac{C}{N} \quad C > 0 \quad (3)$$

where  $N$  is the number of atoms. In this case every particle interacts with the other  $N - 1$  particles with the same strength. This is often interpreted as a model with nearest neighbour interaction in infinite dimension (for  $N \rightarrow \infty$ ). However, to allow comparison with the predictions of [16] we assume a three-dimensional lattice. Thus our choice of  $C_{kl}$  is a special case of that treated in [16]. Of course, infinite-range interactions do not really occur in nature, but they are interesting from a theoretical point of view, e.g. mean field predictions become correct since factorization of higher order *static* correlation functions is exact in that case. MCT factorizes *time-dependent* higher order correlation functions. Therefore one could expect that the mode coupling approximation becomes better for infinite-range interactions. The investigation of this point is part of our motivation. In addition the choice of infinite-range interactions has the advantage that static quantities like the isothermal susceptibility, needed for the MCT, may be obtained analytically and the *equation* for the *non-ergodicity parameter* (ENP)

$$L_q = \lim_{t \rightarrow \infty} S(q, t) \quad (4)$$

can be solved exactly. Here

$$S(q, t) = \sum_n S_{n0}(t) e^{-iqRn}. \quad (5)$$

Non-ergodic behaviour is signalled by  $L_q > 0$  and vanishing  $L_q$  indicates ergodic motion. It is this correlation function we have calculated from molecular dynamical simulations to test ergodicity.

The organization of this article is as follows. The next section will briefly review MCT for the  $\phi^4$ -model and will present the exact solution of the ENP yielding  $L_q(T)$ . The third section contains details and results of the numerical simulation. Finally we will discuss these numerical results with respect to MCT and summarize our findings.

## 2. Mode coupling theory

First, we briefly describe the mode coupling approach used by Aksenov *et al* [16]. This approach is based on the projection operator technique proposed by Tserkovnikov [18] which is equivalent to the Mori-Zwanzig formalism [19]. Starting from the Laplace transform of  $S(q, t)$ :

$$\widehat{S}(q, z) = \mp i \int_{-\infty}^{\infty} dt \theta(\pm t) S(q, t) e^{izt} \quad \text{Im } z \geq 0 \quad (6)$$

where  $\theta(t)$  is the Heaviside function, this technique generates a hierarchy of equations. Using the first two equations of this hierarchy,  $\widehat{S}(q, z)$  can be presented in the familiar form:

$$\widehat{S}(q, z) = \frac{\beta^{-1} \chi_q}{z - [\chi_q(z - \beta B^2 \widehat{M}^{(2)}(q, z))]^{-1}} \quad (7)$$

with  $\beta = 1/k_B T$  and the isothermal susceptibility

$$\chi_q = \beta S(q, t = 0) \equiv \beta S_q. \quad (8)$$

The irreducible part  $\widehat{M}^{(2)}(\mathbf{q}, z)$  of the second-order relaxation kernel involves the anharmonicity of the  $\phi^4$ -model:

$$\widehat{M}^{(2)}(\mathbf{q}, z) = \langle u_k^3(t) u_l^3(0) \rangle^{(2)}(\mathbf{q}, z). \quad (9)$$

Using Tserkovnikov's technique and the Fourier-Laplace transform of the following time correlation functions:

$$\begin{aligned} R_{kl}(t) &= \langle p_k(t) u_l(0) \rangle \\ E_{kl}(t) &= \langle p_k(t) p_l(0) \rangle \\ F_{kl}(t) &= \langle p_k(t) u_l^3(0) \rangle \\ N_{kl}(t) &= \langle u_k^3(t) u_l(0) \rangle \\ M_{kl}(t) &= \langle u_k^3(t) u_l^3(0) \rangle \end{aligned} \quad (10)$$

we find

$$\widehat{M}^{(2)}(\mathbf{q}, z) = \widehat{M}^{(1)}(\mathbf{q}, z) + \widehat{F}^{(1)}(\mathbf{q}, z) [\widehat{E}^{(1)}(\mathbf{q}, z)]^{-1} \widehat{F}^{(1)}(-\mathbf{q}, z) \quad (11a)$$

with

$$\begin{aligned} \widehat{M}^{(1)}(\mathbf{q}, z) &= \widehat{M}(\mathbf{q}, z) - \widehat{N}(\mathbf{q}, z) [\widehat{S}(\mathbf{q}, z)]^{-1} \widehat{N}(-\mathbf{q}, z) \\ \widehat{F}^{(1)}(\mathbf{q}, z) &= \widehat{F}(\mathbf{q}, z) + \widehat{N}(\mathbf{q}, z) [\widehat{S}(\mathbf{q}, z)]^{-1} \widehat{R}(-\mathbf{q}, z) \\ \widehat{E}^{(1)}(\mathbf{q}, z) &= \widehat{E}(\mathbf{q}, z) + \widehat{R}(\mathbf{q}, z) [\widehat{S}(\mathbf{q}, z)]^{-1} \widehat{R}(-\mathbf{q}, z) \end{aligned} \quad (11b)$$

where the symmetry of the functions (10) under time reversal and reflection has been used. On the next level of the hierarchy an equation similar to (7) can be derived for  $\widehat{M}^{(2)}(\mathbf{q}, z)$ . In general this procedure does not stop and leads to an infinite set of coupled equations. An exact solution is therefore impossible, and approximations are unavoidable. The simplest but crudest one is as follows [16]

$$M_{kl}^{(2)}(t) \simeq 6[S_{kl}(t)]^3. \quad (12)$$

The nature of this approximation is best elucidated by adopting the Mori-Zwanzig formalism. If  $\mathcal{P}$  denotes the projection onto the variables  $\{u_k\}$ ,  $\{p_k\}$  and  $\mathcal{L}$  the Liouvillian corresponding to the Hamiltonian  $H$ ,  $\widehat{M}_{kl}^{(2)}(z)$  can be represented as follows [19]:

$$\widehat{M}_{kl}^{(2)}(z) = \langle f_k | [z - Q\mathcal{L}Q]^{-1} | f_l \rangle \quad (13a)$$

with the fluctuating force

$$f_k(t) = \frac{1}{B} Q\mathcal{L}p_k(t) \quad (13b)$$

and

$$Q = 1 - \mathcal{P}. \quad (13c)$$

In the following we always assume  $T > T_c$  which implies  $\langle x_k \rangle = 0$  or  $u_k = x_k$  for all  $k$ . Using this and the equation of motion we obtain

$$\frac{1}{B} \mathcal{L} p_k = i \mathcal{Q} u_k^3 \tag{14}$$

and with (13b)

$$\widehat{M}_{kl}^{(2)}(z) = \langle \mathcal{Q} u_k^3 | [z - \mathcal{Q} \mathcal{L} \mathcal{Q}]^{-1} | \mathcal{Q} u_l^3 \rangle \tag{15a}$$

which is the Laplace transform of

$$M_{kl}^{(2)}(t) = \langle \mathcal{Q} u_k^3(0) e^{-i\mathcal{Q} \mathcal{L} \mathcal{Q} t} \mathcal{Q} u_l^3(0) \rangle \tag{15b}$$

i.e. the time dependence of the *irreducible* part of the second-order kernel is determined by

$$\mathcal{L}^{\mathcal{Q}} = \mathcal{Q} \mathcal{L} \mathcal{Q} \tag{16}$$

the Liouvillian in the space of dynamical variables *orthogonal* to  $\{u_k\}$  and  $\{p_k\}$ . Consequently, approximation (12) consists of two steps, first the replacement

$$\mathcal{L}^{\mathcal{Q}} \rightarrow \mathcal{L} \tag{17}$$

and second the factorization

$$\langle \mathcal{Q} u_k^3(0) e^{-i\mathcal{L} t} \mathcal{Q} u_l^3(0) \rangle \rightarrow 6 \langle u_k(t) u_l(0) \rangle^3. \tag{18}$$

Both steps must be taken together in order to avoid unphysical results [20]. The ENP derived by Aksenov *et al* [16] for the  $\phi^4$ -model and the ENP for supercooled liquids are based on these approximations†. Substitution of (12) into (7) and taking

$$L_{\mathbf{q}} = \lim_{t \rightarrow \infty} S(\mathbf{q}, t) = \lim_{z \rightarrow 0} z \widehat{S}(\mathbf{q}, z) \tag{19a}$$

$$\lim_{t \rightarrow \infty} M_{kl}^{(2)}(t) = \lim_{z \rightarrow 0} z \widehat{M}_{kl}^{(2)}(z) \simeq 6(L_{kl})^3 \tag{19b}$$

into account ( $L_{kl}$  is the Fourier transform of  $L_{\mathbf{q}}$ ) we arrive at the ENP for the  $\phi^4$ -model

$$\frac{l_{\mathbf{q}}}{1 - l_{\mathbf{q}}} = \lambda_{\mathbf{q}} \frac{1}{N^2} \sum_{\mathbf{q}', \mathbf{q}''} l_{\mathbf{q} - \mathbf{q}' - \mathbf{q}''} l_{\mathbf{q}'} l_{\mathbf{q}''} \tag{20a}$$

with

$$l_{\mathbf{q}} = \beta L_{\mathbf{q}} / \chi_{\mathbf{q}} \quad \lambda_{\mathbf{q}} = 6B^2 \chi_{\mathbf{q}}^4 / \beta^2. \tag{20b}$$

The mathematical structure of these equations, first derived in [16], is very similar to the ENP for liquids [8]. Because of the  $\mathbf{q}$ -dependence they can usually only be solved

† See also section 3.4 of [8].

numerically. However, for the model with infinite-range interactions the ENP can be solved exactly in the limit  $N \rightarrow \infty$ . In this case  $\chi_q$  takes only two values:

$$\chi_q = \begin{cases} \chi_0 & q = 0 \\ \chi_1 & q \neq 0 \end{cases} \quad (21)$$

The same is true for  $L_q$ , i.e.

$$L_q = \begin{cases} L_0 & q = 0 \\ L_1 & q \neq 0 \end{cases} \quad (22)$$

Then, in leading order in  $N$ , (20a) reduces to

$$\frac{l_0}{1-l_0} = \lambda_0 l_1^3 \quad (23a)$$

$$\frac{l_1}{1-l_1} = \lambda_1 l_1^3 \quad (23b)$$

where  $\lambda_0, \lambda_1$  are defined analogous to  $\chi_0, \chi_1$  and  $L_0, L_1$ .

Two conclusions can easily be drawn from (23):

(i) for a harmonic on-site potential, i.e.  $B = 0$ , (23) possess only the trivial solution  $l_q = 0$  (of course this is true for (20) too); and

(ii)  $l_1 \neq 0$  implies  $l_0 \neq 0$  and vice versa.

Therefore it is sufficient to discuss (23b). It is easy to show that for

$$\lambda_1 > \lambda_c = 27/4 \quad (24)$$

there exist two positive solutions besides the trivial one. From these two only the larger one is physical (see [8]). At  $\lambda_c$  a discontinuous transition from  $L_q = 0$  to  $L_q > 0$  takes place, called a B-type transition [8]. Equations (24) and (20b) yield an equation for  $T'_c$ :

$$k_B T'_c = \frac{3}{2\sqrt{2}B} \chi_1(T'_c). \quad (25)$$

Using the equations for  $T_c$  and  $T'_c$ , which will be derived in the appendix, it follows that

$$T_c < T'_c \quad \text{for } C/\sqrt{B} < (8/9)^{1/4} \sqrt{k_B T'_c} \quad (26)$$

and  $T_c > T'_c$  otherwise.

But notice that (20) and therefore (23) too, were derived under the assumption that  $\langle x_k \rangle = 0$  which only holds for  $T > T_c$ . To discuss the possibility  $T'_c < T_c$  one has to take  $\langle x_k \rangle \neq 0$  into account.

For  $|\lambda - \lambda_c|$  small, the reduced non-ergodicity parameter  $l_1$  behaves as follows:

$$l_1(\lambda) = \begin{cases} 0 & \lambda < \lambda_c \\ \frac{2}{3} + \frac{4}{27} \sqrt{\lambda - \lambda_c} & \lambda > \lambda_c \end{cases} \quad (27)$$

which describes a *discontinuous* transition with the same square root behaviour as that found for liquids [8].

### 3. Numerical procedure and results

In this section we present some details of our numerical simulations performed to investigate the existence of a kinetic singularity at  $T'_c$ . Instead of calculating  $S_{kl}(t)$  it is numerically more convenient to consider the correlation function:

$$G_{kl}(t) = \langle \sigma_k(t) \sigma_l(0) \rangle - \langle \sigma_k \rangle \langle \sigma_l \rangle \quad (28)$$

of the *coarse-grained* variables (pseudo-spins):

$$\sigma_k(t) = \text{sgn}(x_k(t)) \quad (29)$$

(cf [15] and especially [17]). An arrest of the fluctuations of  $u_k(t)$  at  $T'_c$  will imply the freezing of the fluctuations of  $\sigma_l(t)$ , leading to a long time tail for  $G_{kl}(t)$ , i.e. it is

$$K_q = \lim_{t \rightarrow \infty} G_q(t) > 0 \quad (30)$$

for  $T < T'_c$  provided the prediction of [16] is correct. Since (30) holds for *all*  $q$  it is sufficient to investigate the autocorrelation function  $G_{kk}(t)$  in order to prove or disprove the existence of a non-ergodic instability. Therefore we have solved numerically the equations of motion

$$\frac{d^2 y_k}{dt'^2} + y_k(y_k^2 - 1) = \frac{\mu}{N} \sum_{n=1}^N y_n \quad k = 1, \dots, N \quad (31)$$

for the infinite-range model and different  $N$ .  $y_k, t'$  and  $\mu$  are rescaled variables:

$$\begin{aligned} y_k &= \left( \frac{A-C}{B} \right)^{-1/2} x_k \\ t' &= \left( \frac{A-C}{m} \right)^{1/2} t \\ \mu &= \frac{C}{A-C}. \end{aligned} \quad (32)$$

Note that  $A - C$  is positive, due to the restriction to the order-disorder regime and that  $y_k$  is the rescaled displacement from a three-dimensional lattice point  $\mathbf{R}_k$ .

In the molecular dynamics simulations we have integrated (31) with the velocity form of the Verlet algorithm [21] for different system sizes  $N$  between 100 and 3000. We usually employed a step size  $h = 0.02$  tu (rescaled time units) except for several runs with  $h = 0.01$  tu to test the dependence of our results on  $h$ . We found no dependence on  $h$ . This time step leads to relative fluctuations in the total energy of order  $10^{-5}$  over the whole run and a relative drift in temperature of less than 1%. To set up the initial configurations of the system in phase space we chose  $N$  Gaussian distributed random numbers with mean values between 0.8 and 1.0 and width between 0.5 and 1.0. Changing the sign of about half of these numbers randomly (to occupy the left and right well of  $V_0(x)$  with equal probability) they were used as initial displacements  $y_k(0)$ . Similarly, the initial velocities  $\dot{y}_k(0)$  were generated from



$N$  Gaussian distributed random numbers with mean zero and width between 0.6 and 1.0.

We equilibrated the system by rescaling the velocities of all the particles at every time step [22]. This was done for at least 10% of the total run length but for large systems and low temperatures up to 30% of the total time. Longer equilibration times for larger systems were required because the fluctuations of the right-hand side (31) decrease with increasing  $N$  (and thus the effective coupling between the particles decreases). We found to a good approximation that the RMS of the right-hand side of (31) behaves like  $N^{-1/2}$  (see figure 1) independent of temperature for the investigated range  $T > T_c$ .

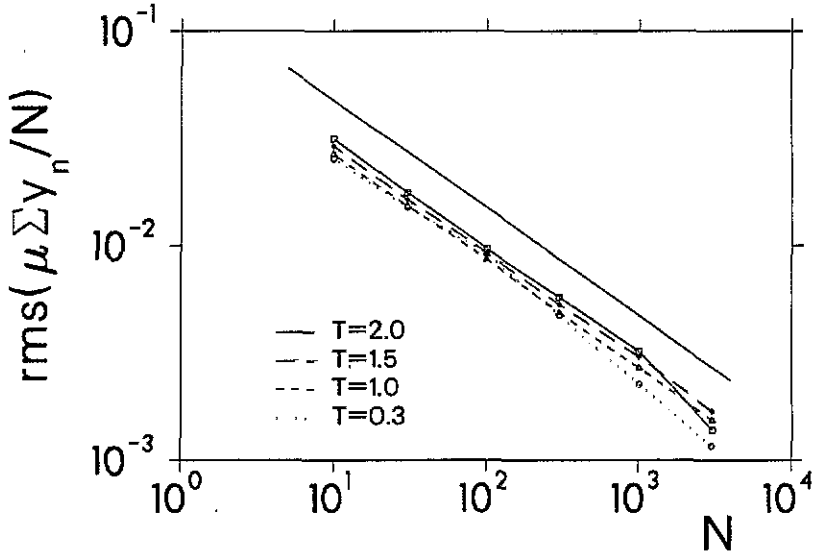


Figure 1. Root-mean-square of  $\mu \sum y_n(t)/N$  as a function of system size for different temperatures. The straight line corresponds to  $N^{-1/2}$ .

To reduce the scattering of the data for  $G_{kk}(t)$  we have calculated

$$\bar{G}_{kk}(t) = \frac{1}{N} \sum_{k=1}^N G_{kk}(t) \tag{33}$$

which is shown in figure 2 for different  $N$  and  $\mu = 0.08$ . For some temperatures the relaxation behaviour is given over 4 to almost 6 orders of magnitude, thus ranging from microscopic to mesoscopic time scales. Since the time averaging on the two time scales had to be done separately, the two regimes do not match perfectly. But the discrepancy, which is a measure of the accuracy of our numerical simulations, decreases with increasing  $N$ . Qualitatively similar results to those shown in figure 2 were found also for  $\mu = 0.215$ .

On the microscopic time scale, over tens of Einstein periods (equal to  $2\pi \tau_u$ ), oscillations occur which become damped afterwards and lead to a plateau on a logarithmic scale. Surprisingly the appearance of such a plateau has also been found for the density correlation function of two- and three-component liquids [10]. In our case the length of the plateau increases with  $N$ , as demonstrated in figure 3.

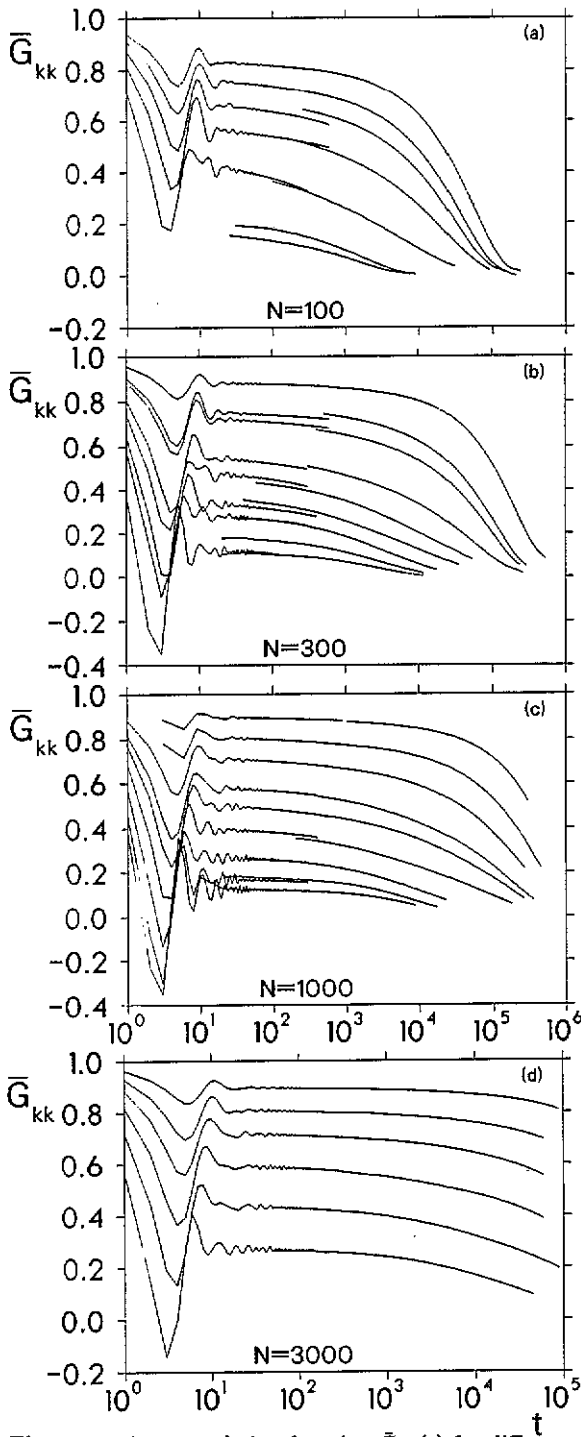


**Figure 2.** Autocorrelation function  $\bar{G}_{kk}(t)$  for different temperatures for  $\mu = 0.08$  and different system sizes. (a)  $N = 100$  and temperature from top to bottom: 0.11, 0.2, 0.3, 0.4, 0.6, 1.5, 2.0. (b)  $N = 300$  and  $T = 0.11, 0.15, 0.2, 0.3, 0.4, 0.5, 0.7, 1.0, 1.5, 2.0$ . (c)  $N = 1000$  and  $T = 0.11, 0.15, 0.2, 0.3, 0.4, 0.6, 1.0, 1.5, 2.0$ . (d)  $N = 3000$  and  $T = 0.11, 1.15, 0.2, 0.3, 0.5, 1.0$ .

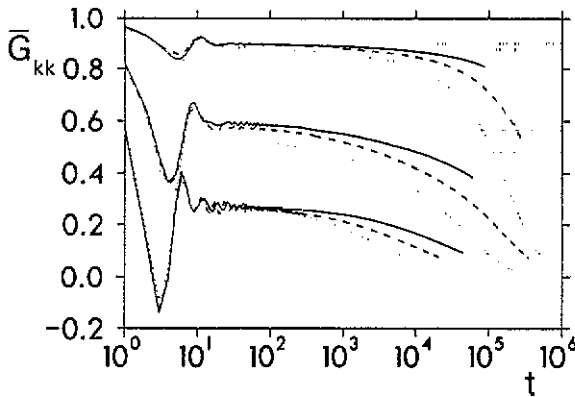


Figure 3.  $\bar{G}_{kk}(t)$  for different system sizes and temperatures.  $\mu = 0.08$ : full curve,  $N = 3000$ ; broken curve,  $N = 1000$ ; dotted curve,  $N = 300$ . Temperatures from top to bottom: 0.11, 0.3, 1.0.

We have analysed the relaxation functions  $\bar{G}_{kk}(t)$  with respect to the temperature dependence of both the mean relaxation time  $\tau(T)$  and the stretching of relaxation times quantified by the Kohlrausch-exponent  $\beta(T)$  and finally we explored the existence of a dynamical transition.

### 3.1. Relaxation time and stretching

To compute the mean relaxation time and determine a measure for the stretching, we fit  $\bar{G}_{kk}(t)$  with a Kohlrausch-Williams-Watts (KWW) law:

$$\hat{G}_{kk}(t) = A \exp[-(t/\tau)^\beta]. \quad (34)$$

Although the KWW law fits our data on the mesoscopic time scale quite well, our results are not necessarily a proof for a KWW law, since the time range scaled with  $\tau(T)$  is rather short. Therefore the KWW-exponent  $\beta(T)$  should only be considered as a *measure of stretching*. An Arrhenius plot for  $\tau(T)$  is shown in figure 4 for different  $N$  and two different  $\mu$  values.  $\tau(T)$  reveals a rather unusual behaviour. Whereas an Arrhenius law may exist for higher temperatures, the relaxation behaviour relative to this law gets *accelerated* for lower temperatures (but still sufficiently above the critical temperature  $T_c$ ) in contrast to all systems (known to us) undergoing a liquid-glass transition (cf a plot proposed by Angell for the viscosity  $\eta$  as function of  $T_g/T$  [23] and assume  $\tau \sim \eta$ ). Approaching  $T_c$  the mean relaxation time will increase very rapidly leading to a divergency at  $T_c$  (critical slowing down). This regime has not been explored by us. We stress that the result for  $\tau(T)$  looks quite similar to that in figure 4 if one uses the area under the relaxation curve as a relaxation time. This demonstrates that the assumption that  $\hat{G}_{kk}(t)$  follows a KWW law is not critical for the conclusions stated in this paragraph. Note also that  $\tau(T)$  does not reveal any singularity at  $T'_c \simeq 1.05$  (for the calculation of  $T'_c$  see the appendix) as predicted by the MCT.

The corresponding KWW-exponent  $\beta$  is presented in figure 5. Although the data for different initial configurations scatter, the  $T$  dependence of  $\beta$  is reasonably well defined.

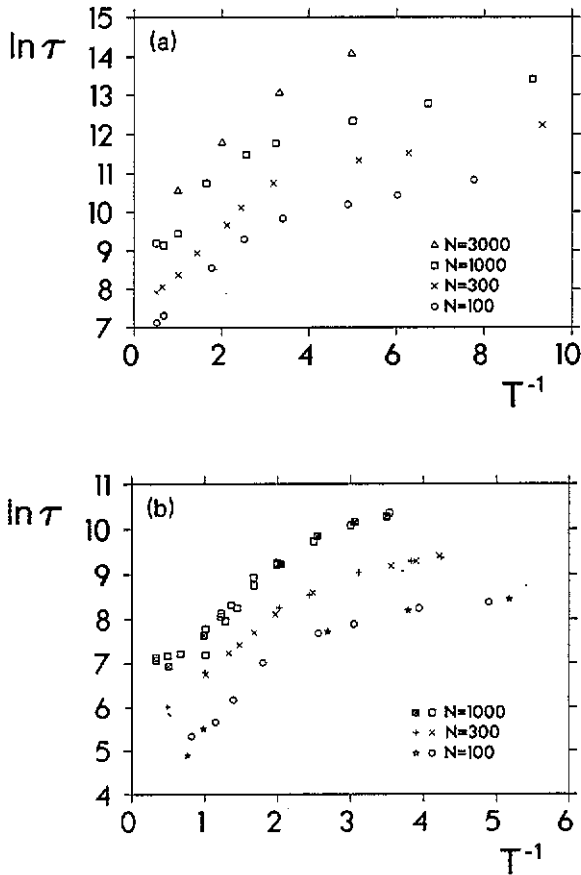


Figure 4. Arrhenius-plot for the relaxation time  $\tau$  for different system sizes. (a)  $\mu = 0.08$ ,  $1/T_c \approx 13.8$ ; (b)  $\mu = 0.215$ ,  $1/T_c \approx 5.58$ . The different symbols for the same values of  $N$  in (b) denote different initial conditions.

There is a *minimum* between 0.5 and 1.0. For  $T$  approaching zero or infinity  $\beta$  seems to converge to unity. Since  $1 - \beta$  can be considered as a measure of cooperativity one may thus conclude that the cooperative motion of the particles is maximum between  $T = 0.5$  and  $T = 1.0$ .

### 3.2. Non-ergodicity parameter

Analogous to the liquid-glass transition, we do *not* expect an ideal dynamical transition for the  $\phi^4$ -model due to the existence of hopping transitions at least for finite  $N$  (see also the first paragraph of section 4.2). Therefore we anticipate that in this case  $K_q \equiv 0$ . Nevertheless it might be possible to deduce a non-ergodicity parameter from the relaxation behaviour compatible with the MCT results, (25). This may be feasible due to a *quasi* non-ergodic behaviour leading to a plateau in the relaxation function. Therefore, similar to the analysis of some of the experimental data [9], we fit our data with a KWW law and use as a (quasi)-non-ergodicity parameter  $Q_0$  the amplitude  $A(T)$ .  $A(T)$  is given roughly by the value of the plateau appearing in  $\hat{G}_{kk}(t)$  and is shown in figure 6.  $A(T)$  does not exhibit any evidence for a dynamical transition or

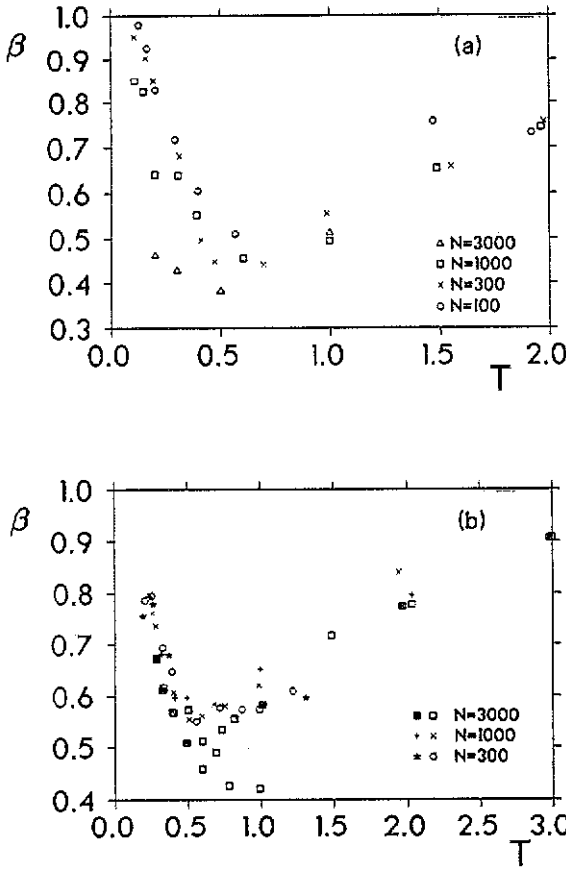


Figure 5. kww-exponent  $\beta$  as a function of temperature for different system sizes. (a)  $\mu = 0.08$ ; (b)  $\mu = 0.215$ . The different symbols for the same values of  $N$  in (b) denote different initial conditions.

cross-over at  $T'_c \simeq 1.05$ .

Remember that for  $T > T_c$  and  $N$  large the fluctuations of the right-hand side (31) are of order  $N^{-1/2}$  and therefore can be approximated by zero, at least for times  $t$  smaller than a certain time  $t_0(N)$ . Therefore let us consider  $N = \infty$  for a moment. In this case the interactions may be neglected completely. Hence the energy of each atom is conserved implying non-ergodicity. This has been already mentioned by Onodera and recently by Flach [24]. In this case the non-ergodicity parameter  $Q_0(T)$  can easily be determined.  $Q_0(T)$  is just the relative mean number of particles with energy smaller than the single-particle barrier, because for these particles  $\sigma_k(t)\sigma_k(0) = 1$  for all times. Using the rescaled variables (32) and the corresponding one-particle Hamiltonian:

$$\bar{H}_0(p, y) = \frac{1}{2}p^2 + \bar{V}_0(y) \tag{35a}$$

with

$$\bar{V}_0(y) = -\frac{1}{2}y^2 + \frac{1}{4}y^4 \tag{35b}$$

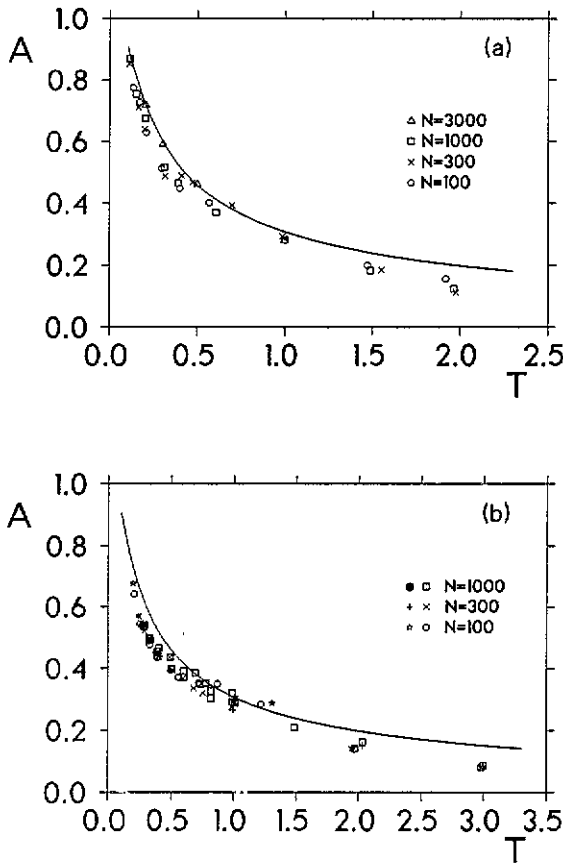


Figure 6. Amplitude  $A(T)$  of the KWW fit as a function of temperature for different system sizes. For the full curve see text. (a)  $\mu = 0.08$ ; (b)  $\mu = 0.215$ .

it follows

$$Q_0 = \frac{1}{Z_0} \int_{\bar{H}_0(p,y) \leq 0} dp \int dy e^{-\beta \bar{H}_0(p,y)} \quad (36a)$$

with

$$\bar{Z}_0 = \int_{-\infty}^{\infty} dp \int_{-\infty}^{\infty} dy e^{-\beta \bar{H}_0(p,y)}. \quad (36b)$$

The integrals appearing in (36) have been evaluated numerically leading to the result for  $Q_0(T)$  presented by the full curve in figure 6. Note that  $Q_0(T)$  varies smoothly with  $T$ , without any distinguished temperature. This figure demonstrates reasonable agreement between the exact result for  $Q_0$  in the case  $C = 0$  and the numerical one for the finite and interacting system. We will return to this point in the next section.

#### 4. Discussion of the results

This section will mainly discuss the numerical results for the autocorrelation function  $\bar{G}_{kk}(t)$  in the spirit of MCT. First we consider the  $T$  dependence of the mean relaxation time  $\tau$  and the KWW-exponent  $\beta$ .

#### 4.1. Relaxation time and stretching

The concave curvature for  $\tau(T)$  shown in figure 4 signifies a decrease in the relevant barriers with decreasing temperature. That this really happens for the infinite-range model has been proved recently by Ovchinnikov and Onishyk [25]. These authors show the existence of a critical value  $\mu_c = \frac{1}{3}$  at which the general appearance of the energy landscape in configuration space, e.g. the barrier heights, changes qualitatively. In particular they argue that the relaxation is accelerated or decelerated for  $\mu$  smaller or larger than  $\mu_c$ , respectively. This demonstrates that the relaxation behaviour is intimately related to the qualitative properties of the energy landscape and it is an interesting and probably difficult challenge to have a more general understanding of this relationship from a microscopic point of view [23].

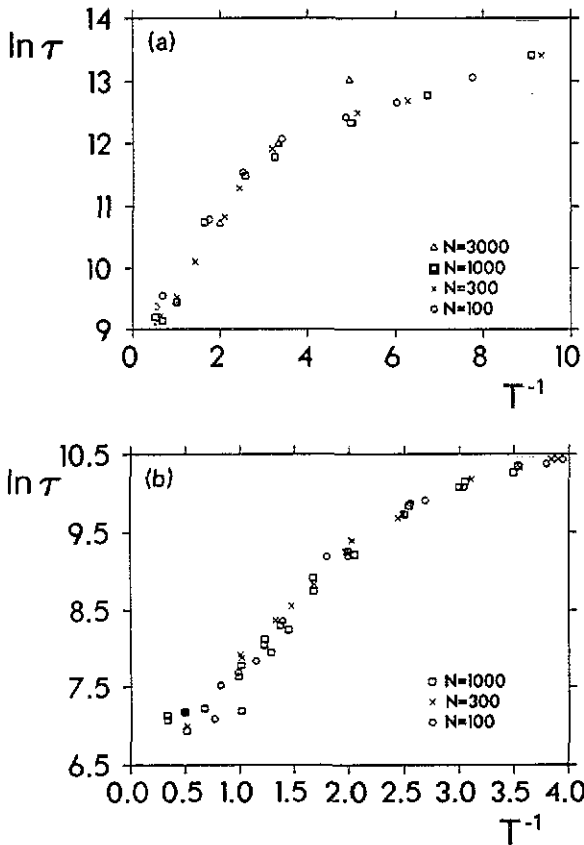


Figure 7. Relaxation time  $\tau$  scaled with  $N^\alpha$ . (a)  $\mu = 0.08$ ,  $\alpha = 0.97$ ; (b)  $\mu = 0.215$ ,  $\alpha = 0.95$ .

Another interesting feature of  $\tau(T)$  is its  $N$  dependence. Since the  $\tau$  against  $T$  curves for different  $N$  in figure 4 seem to be just shifted, it is tempting to check the validity of a scaling law for  $N \gg 1$ :

$$\tau(T, N) = N^\alpha \tau_0(T). \quad (37)$$

Using the results given in figure 4 we determined  $\alpha$  by maximizing  $(1 - r_s)^2$  where  $r_s$  is the Spearman rank-order correlation coefficient (see, for example, [26]). The results of this non-parametric fit are presented in figure 7. Apart from some scattering at higher temperatures all our data seem to fall onto one curve†. From this scaling we obtain:  $\alpha = 0.97 \pm 0.03$  for  $\mu = 0.08$  and  $\alpha = 0.95 \pm 0.03$  for  $\mu = 0.215$ . Probably the correct value is  $\alpha = 1$ , provided the scaling ansatz is correct. Of course, the  $N$  dependence of  $\tau$  is due to the infinite range of the interactions. But the  $T$  dependence of  $\tau_0$  may resemble that for a system with short-range interactions, e.g. critical slowing down should occur:  $\tau_0 \rightarrow \infty$  for  $T \rightarrow T_c$ .

The main conclusion following from figure 5 is the  $T$  dependence of the KWW-exponent  $\beta$ . This is in contrast to the time-temperature superposition principle valid for supercooled liquids [8]. In particular the stretching is maximum for  $T$  between 0.5 and 1. In this range  $T$  is of the order of  $E_b = 0.25$ , the barrier height of  $\hat{V}_0$  when expressed in scaled variables.

#### 4.2. Non-ergodicity-parameter

The numerical data shown in figure 6 for the amplitude  $A(T)$  of the KWW law do not reveal any sign of an underlying singularity. Although simulation results do not constitute a rigorous proof, we think that the smoothness of  $A(T)$  at  $T_c'$  rules out any signature of a dynamical transition. The agreement between these data and the analytical result for the non-ergodicity parameter  $Q_0$ , when the interactions are neglected, allows the following physical interpretation: for finite  $N$ , those particles with energy smaller than the single-particle barrier stay in the well where they have been at  $t = 0$  and oscillate around their local minimum. This will be true for  $t \ll t_0(N)$  and may be compared with the *cage effect* for supercooled liquids [8]. For times comparable with or larger than  $t_0(N)$  the interaction will come into play, leading to transitions (hopping) between both local minima and restoring ergodicity. Thus  $1/N$  may be compared with the parameter  $\delta$  describing the hopping processes in liquids [8]. This interpretation can be used for short-range interactions as well, but with  $\delta$  being finite and independent on  $N$ . For  $N = \infty$  ergodicity is really broken, however, for *all* temperatures. This is in disagreement with the result by Aksenov *et al.* We now investigate this discrepancy.

Equation (11) allows us to express  $\widehat{M}^{(2)}$  in terms of  $\widehat{E}, \widehat{F}, \widehat{N}, \widehat{R}, \widehat{S}$  and  $\widehat{M}$ . These quantities are not independent. Using the equations of motion ( $m = 1$ ):

$$\begin{aligned} \dot{u}_k &= p_k \\ \dot{p}_k &= D_{kl} u_l - B u_k^3 \end{aligned} \quad (38a)$$

with

$$D_{kl} = \left( A - \sum_j C_{0j} \right) \delta_{kl} + C_{kl} \quad (38b)$$

we find for the time-correlation functions (10) the equations of motion:

$$\dot{\hat{S}}_{kl} = R_{kl}$$

† The point  $N = 3000$  at  $1/T \simeq 5.0$  in figure 7(a) has a large error bar and does not contradict this statement.



$$\begin{aligned}
 \dot{R}_{kl} &= -E_{kl} = D_{km}S_{ml} - BN_{kl} \\
 \dot{E}_{kl} &= -D_{km}R_{ml} - BF_{kl} \\
 \dot{F}_{kl} &= -N_{km}D_{ml} + BM_{kl} \\
 \dot{N}_{kl} &= -F_{kl}.
 \end{aligned}
 \tag{39}$$

Note that we assume  $\langle x_k \rangle = 0$  in (38a), since only  $T > T_c$  is considered in this paper. Furthermore summation over repeated indices is understood. Taking the Fourier-Laplace transform of these equations and using (11) we find

$$z\widehat{M}^{(2)}(\mathbf{q}, z) \rightarrow z\widehat{M}(\mathbf{q}, z) - D_{\mathbf{q}}/B)^2 L_{\mathbf{q}} + (\beta B)^{-2} L_{\mathbf{q}}/[S_{\mathbf{q}}(S_{\mathbf{q}} - L_{\mathbf{q}})] \tag{40}$$

for  $z \rightarrow 0$ . Substituting this into (7) it follows that

$$z\widehat{M}(\mathbf{q}, z) \rightarrow (D_{\mathbf{q}}/B)^2 L_{\mathbf{q}} \tag{41}$$

for  $z \rightarrow 0$ . Expression (41) can be derived without using any projection techniques since (39) allow us to deduce an equation only involving  $S_{kl}^{(4)}(t), S_{kl}^{(2)} \equiv S_{kl}(t), S_{kl}(t)$  and  $M_{kl}(t)$ . The Fourier-Laplace transform of this equation and the limit  $z \rightarrow 0$  immediately yields (41). Using the Gaussian approximation (for  $T > T_c$ )

$$M_{kl}(t) \simeq 6(S_{kl}(t))^3 + 9\langle u_k^2 \rangle^2 S_{kl}(t) \tag{42}$$

equation (41) yields for the scaled variables (32) and the infinite-range model

$$(1 - 9\langle y_k^2 \rangle^2)L'_0 = 6L'_1{}^3 \tag{43a}$$

$$(1 - 9\langle y_k^2 \rangle^2)L'_1 = 6L'_1{}^3 \tag{43b}$$

where  $L'_{\mathbf{q}} = (A - C)L_{\mathbf{q}}/B$ , the rescaled non-ergodicity parameter. Similar to (23) we obtain a non-trivial solution

$$L'_1 = \sqrt{(1 - 9\langle y_l^2 \rangle^2)/6}. \tag{44}$$

$\langle y_k^2 \rangle(T)$  can be evaluated numerically as a function of  $T$ . The function has a minimum with a value larger than 0.830. Therefore the square root is always imaginary, i.e. there is no non-trivial solution and therefore no instability. Although the quality of approximation (42) is unclear (as is the case for approximation (12)), in our model it eliminates the instability and is therefore consistent with our numerical finding. However, the Gaussian approximation has another drawback since it implies  $L_{\mathbf{q}} = 0$  which is unphysical for the infinite-range model. This is not surprising due to the double-well character of the on-site potential playing a role even above  $T_c$ . This demonstrates how crucial the approximations can be.

## 5. Summary

First of all let us repeat the results obtained by Aksenov *et al* [16]. For a three-dimensional  $\phi^4$ -model an equation for the non-ergodicity parameter  $L_q$  (which is (20) in our paper) was derived within the MCT for an *arbitrary* range of interactions. This should hold for infinite-range interactions as well. However, our intensive numerical simulations do not yield any evidence for a non-ergodic instability, not even for a smeared out version. This is supported by the smooth temperature dependence of the height of the plateau (found for the autocorrelation function for the infinite-range model) which has been interpreted as a non-ergodicity parameter for the finite system. This interpretation has been strengthened by the reasonable agreement between this height and the exact non-ergodicity parameter of the non-interacting system. The latter system is obviously non-ergodic, due to the double-well character of the on-site potential breaking the 'left-right' symmetry for energies smaller than the single-particle barrier. Although this is no longer true in the displacive regime, ergodicity will nevertheless also be broken if the interactions vanish.

Despite these results for the  $\phi^4$ -model, our conclusions cannot be transferred to the MCT for liquids. We stress that the approximations made for liquids using the MCT may be much less crucial which seems to be confirmed by the agreement between numerical and experimental results with some of the predictions of the MCT for supercooled liquids. Nevertheless it is important to learn more for what kind of systems the approximations are reasonable. This knowledge is necessary in order to understand why even several glass forming systems, e.g. vitreous silica, are not in accordance with MCT since, e.g., its viscosity is purely Arrhenius-like above  $T_g$ . Whether this relates only to the neglect of hopping processes and not partially to the mode coupling approximation remains unclear.

We also mention that the accelerated nature found for the temperature dependence of the mean relaxation time  $\tau$  is rather unusual. It proves that the relevant barriers decrease with decreasing temperature (energy), in agreement with recent results by Ovchinnikov *et al* for  $\mu < \frac{1}{3}$  [25]. It would be interesting to have more insight into the relationship between relaxation behaviour of disordered structures and their energy landscape in configuration space as suggested by Angell [23]. Finally, our numerical results exhibit a maximum stretching of relaxation times for a temperature range of the order of  $E_b$ , the barrier of the on-site potential. For temperatures converging to zero or infinity they seem to indicate pure Debye relaxation.

## Acknowledgments

One of us (RS) gratefully acknowledges stimulating discussions with K Binder which have led to these investigations and thanks J Schreiber for comments with respect to the MCT. WK thanks R Della Valle for pointing out to him the idea of the Spearman-rank correlation coefficient. In addition we acknowledge the permission to use the Cray XMP from the ETH in Zürich, the Convex from the Paul Scherrer Institut and the resources of the Computing Center of the University of Basel. Part of this work was supported by the Swiss National Science Foundation.

Appendix

In the following we sketch how to calculate the critical temperature  $T_c$ , the isothermal susceptibility  $\chi_{kl}$  and the temperature  $T'_c$  for the dynamical glass transition for the model given by (1) in the case  $C_{kl} = C/N$ .

Consider the Hamiltonian

$$H = \sum_l h_l x_l \tag{A1}$$

where  $H$  is given by (1) and  $h_l$  denotes the conjugate field with respect to coordinate  $x_l$ . The configuration part of the partition function can be written as

$$Z_c(\mathbf{h}) = \int_{-\infty}^{\infty} dy \int_{-\infty}^{\infty} \prod_l dx_l \exp \left\{ -\beta \sum_l V_l(x_l) + \beta \sum_l h_l x_l + \frac{\beta C}{2N} y^2 \right\} \delta \left( y - \sum_l x_l \right) \tag{A2}$$

where  $\mathbf{h} = \{h_1, \dots, h_n\}$  and

$$V_l(x) = -\frac{A-C}{2} x^2 + \frac{B}{4} x^4. \tag{A3}$$

Using an integral representation of the  $\delta$ -function  $Z_c(\mathbf{h})$  can be written as

$$Z_c(\mathbf{h}) = \frac{1}{2\pi} \int_{-\infty}^{\infty} ds \int_{-\infty}^{\infty} dy \exp \left\{ \frac{\beta C}{2N} y^2 + isy + \sum_l \ln \int_{-\infty}^{\infty} dx_l \exp[-\beta V_l(x_l) - isx_l + \beta h_l x_l] \right\}. \tag{A4}$$

For  $N \rightarrow \infty$  the  $s$ -integration in (A4) can be performed by exploiting the method of steepest descent. This and the relation

$$\chi_{kl} = \frac{1}{\beta} \left[ \frac{\partial}{\partial h_l} \left( \frac{1}{Z_c(\mathbf{h})} \frac{\partial Z_c(\mathbf{h})}{\partial h_k} \right) \right] \Big|_{\mathbf{h} = 0}. \tag{A5}$$

yields for the susceptibility (up to order  $O(1/N)$ )

$$\chi_{kk} = \frac{\beta A_2}{A_0} \tag{A6a}$$

$$\chi_{kl} = \frac{\beta A_2}{N A_0} \frac{1}{(A_0/C\beta A_2) - 1} \quad k \neq l \tag{A6b}$$

with

$$A_i = \int_{-\infty}^{\infty} dx \exp[-\beta V_1(x)] x^i. \tag{A6c}$$

The Fourier transform  $\chi_q$  of  $\chi_{ki}$  is given by

$$\chi_{q=0} = \frac{\beta A_2}{A_0(1 - (\beta C A_2/A_0))} \equiv \chi_0 \quad (A7a)$$

$$\chi_{q \neq 0} = \frac{\beta A_2}{A_0} \equiv \chi_1. \quad (A7b)$$

Equation (A7a) shows that the critical temperature  $T_c$  can be determined from the condition

$$\frac{C\beta_c A_2(\beta_c)}{A_0(\beta_c)} = 1. \quad (A8)$$

From (20b), (24) and (A7b) we arrive at the equation for  $T'_c$

$$\frac{\beta_c'^2 B^2 A_2^4(\beta_c')}{A_0^4(\beta_c')} = \frac{9}{8}. \quad (A9)$$

Choosing scaled variables (32) one immediately finds that (A9) does *not* depend on any of the parameters  $A, B$  and  $C$ . The solution of (A9) (in rescaled units) is given by  $T'_c = 1.05212\dots$ , independent on  $\mu$ .

## References

- [1] Jäckle J 1986 *Prog. Phys.* **49** 171
- [2] Geszti T 1983 *J. Phys. C: Solid State Phys.* **16** 5805  
Leutheusser E 1984 *Phys. Rev. A* **29** 2765  
Bengtzelius W, Götze W and Sjölander A 1984 *J. Phys. C: Solid State Phys.* **17** 5915  
Das S P, Mazenko G F, Ramaswamy S and Toner J J 1985 *Phys. Rev. Lett.* **54** 118  
Kirkpatrick T 1985 *Phys. Rev. A* **31** 939
- [3] Kawasaki K 1976 *Phase Transitions and Critical Phenomena* ed C Domb and M S Green (London: Academic)
- [4] Arnold V I and Avez A 1968 *Ergodic Problems in Classical Mechanics* (New York: Benjamin)
- [5] Das S P and Mazenko G F 1987 *Phys. Rev. A* **34** 2265  
Götze W and Sjögren L 1987 *Z. Phys. B* **65** 415
- [6] Siggia E 1985 *Phys. Rev. A* **32** 3135  
Jäckle J 1989 *J. Phys.: Condens. Matter* **1** 267
- [7] Das S P, Mazenko G F, Ramaswamy S and Toner J 1985 *Phys. Rev. A* **32** 3139
- [8] Götze W 1990 *Liquids, Freezing and the Glass Transition* ed. J P Hansen, D Levesque and J Zinn-Justin (Amsterdam: North-Holland)
- [9] Mezei F, Knaak W and Farago B 1987 *Phys. Rev. Lett.* **58** 571  
Fujara F and Petry W 1987 *Europhys. Lett.* **4** 921  
Frick B, Richter D, Petry W and Buchenau U 1988 *Z. Phys. B* **70** 73  
van Megan W 1989 *Physica A* **157** 705  
Frick B, Farago B and Richter J D 1990 *Phys. Rev. Lett.* **64** 2921  
Rössler E 1990 *Phys. Rev. Lett.* **65** 1595
- [10] Ullo J J and Yip S 1985 *Phys. Rev. Lett.* **54** 1509  
Roux J N, Barrat J-L and Hansen J P 1989 *J. Phys.: Condens. Matter* **1** 7171  
Signorini G F, Barrat J-L and Klein M L 1990 *J. Chem Phys.* **92** 1294  
Brakkee M J D and de Leeuw S W 1990 *J. Phys.: Condens. Matter* **2** 1294  
Wahnström G 1990 *Preprint* (Chalmers University of Technology, Göteborg, Sweden)

- Lewis L J 1990 *Preprint* (Université de Montréal, Montréal, Canada)
- [11] Fredrickson G H and Andersen H C 1984 *Phys. Rev. Lett.* **58** 2091  
— 1985 *J. Chem. Phys.* **8** 5822
- [12] Kirkpatrick T R and Thirumalai D 1987 *Phys. Rev. Lett.* **58** 2091  
— 1987 *Phys. Rev. B* **36** 5388  
— 1988 *Phys. Rev. B* **37** 5342
- [13] Michel K H 1986 *J. Chem. Phys.* **84** 3451  
— 1987 *Z. Phys. B* **68** 259  
— 1988 *Z. Phys.* **71** 369
- [14] Fredrickson G H and Brawer S A 1986 *J. Chem. Phys.* **84** 3351  
Leutheusser E and De Raedt H 1986 *Solid State Commun.* **57** 457
- [15] Bruce A D and Cowley R A 1980 *Adv. Phys.* **29** 1,111,219
- [16] Aksenov V L, Bobeth M, Plakida N M and Schreiber J 1987 *J. Phys. C: Solid State Phys.* **20** 375
- [17] Kob W and Schilling R 1990 *Phys. Rev. A* **42** 2191
- [18] Tserkovnikov Y A 1981 *Teor. Mat. Fiz.* **49** 219
- [19] Forster D 1975 *Hydrodynamic Fluctuations, Broken Symmetry and Correlation Functions* (New York: Benjamin)
- [20] Lovesey S W 1986 *Condensed Matter Physics: Dynamic Correlations* 2nd edn (New York: Benjamin) p 174
- [21] Swope W C, Andersen H C, Berens P H and Wilson K R 1982 *J. Chem. Phys.* **76** 637  
Heerman D W 1986 *Computer Simulation Methods in Theoretical Physics* (Berlin: Springer)
- [22] Woodcock L V 1971 *Chem. Phys. Lett.* **10** 257
- [23] Angell C A 1988 *J. Phys. Chem. Solids* **49** 863
- [24] Onodera Y 1970 *Prog. Theor. Phys.* **44** 1477  
Flach S 1991 *Z. Phys. B* **82** 419
- [25] Ovchinnikov A A and Onishyk V A 1990 *Physica A* **167** 756
- [26] Press W H, Flannery B P, Teukolsky S A and Vetterling W T 1990 *Numerical Recipes in Fortran* (Cambridge: Cambridge University Press)